



Design and Gait Control of an Active Lower Limb Exoskeleton for Walking Assistance

Lingzhou Yu¹(✉), Harun Leto¹, André d'Elbreil², and Shaoping Bai¹

¹ Department of Materials and Production, Aalborg University, Aalborg, Denmark
liyu@mp.aau.dk

² Department of Robotics, École Centrale de Nantes, Nantes, France

Abstract. This paper presents an assistive lower-limb exoskeleton (ALEXO) for active walking assistance. The mechatronics design covering mechanical design, sensors selection and motor controllers are introduced. A 2-link model is built for dynamic analysis control purposes, upon which a trajectory tracking control method based on an improved computed torque control is proposed. This control method was tested with sensor data acquired from walking trials of a healthy subject, which validated the design and gait control of this exoskeleton.

Keywords: active lower-limb exoskeleton · walking gait · trajectory tracking · exoskeleton validation

1 Introduction

Lower-limb exoskeleton technology has advanced significantly for broad applications [1–8]. Most of these devices can be divided into three main lower-limb categories: industry, healthcare and military exoskeletons. Of these, assistive exoskeletons can help patients with stroke and spinal cord injuries to restore their movement abilities [6,7]. Up to date, different exoskeletons have been designed [8–13]. A few exoskeletons use hydraulic actuators, which can obtain high bandwidth, but the system stability is limited by the hydraulic fluid and the servo-valves [14]. Some exoskeletons adopt artificial pneumatic muscles, which are more flexible, but the force bandwidth of the whole system is low [15]. Most exoskeletons use electric motors, for example, the Hybrid assistive limb(HAL) exoskeleton, which can provide walking assistance for hemiplegia patients [16].

For achieving active assistance, control methods have to be developed to meet the needs of different tasks. In [17], an adaptive algorithm was proposed for a rehabilitation exoskeleton. The dynamic movement primitives(DMP) control method was applied to an exoskeleton for human power augmentation [18]. To generate a reasonable reference actuator torque for a flexible gait pattern, a central pattern generator (CPG) was utilized in [19] to produce continuous gait trajectory. A hybrid controller using CPG and admittance controller with electromyography (EMG) signals has achieved trajectory generating for both hip and knee joints [20]. In spite of these developments, control methods that are

able to achieve efficient walking assistance on active lower exoskeletons are still a major challenge.

In this paper, a design of an active lower-limb exoskeleton robot (ALEXO) is proposed for walking assistance. The exoskeleton was designed with a lightweight structure, which is suitable for users of different sizes. The sensors and control units are integrated. A computed torque control method is implemented for tracking trajectory.

The remainder of the paper is organized as follows. Section 2 introduces the concept of the exoskeleton, and Sect. 3 describes the control method. Sections 4 and 5 present the results of the simulation and the experimental results with users. The work is concluded in Sect. 6.

2 Active Lower Limb Exoskeleton Robot

2.1 The ALEXO Configuration

The concept of the ALEXO is shown in Fig. 1, which was developed on the basis of the lower-limb module of the full-body exoskeleton AXO-SUIT [21, 22].

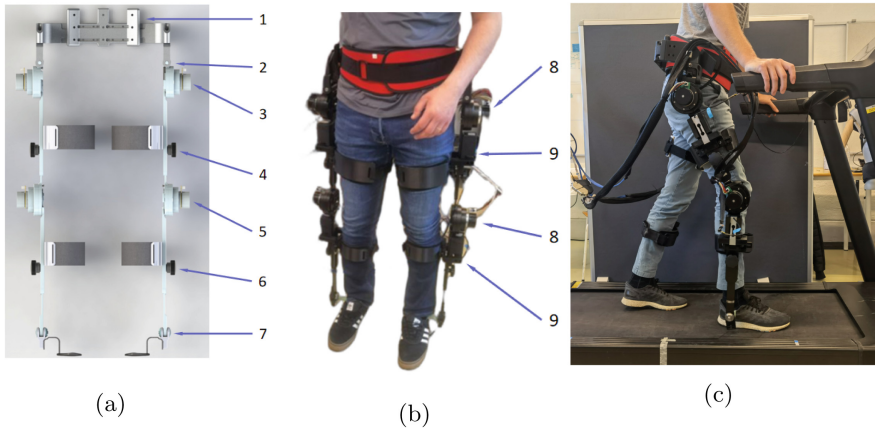


Fig. 1. Concept of ALEXO. (a) The CAD model, (b) the physical system, (c) human-exoskeleton interaction test. The system includes: 1. waist support, 2. passive adduction/abduction hip joint, 3. active flexion/extension hip joint, 4. thigh adjustment screw, 5. active flexion/extension knee joint, 6. shank adjustment screw, 7. passive plantar flexion/dorsiflexion ankle joint, 8. harmonic drive unit driven by EC60 100W brushless motors, 9. Forsentek FNG30 load sensors.

The ALEXO was designed to help individuals with walking difficulty by enhancing the lower limbs' motion in sagittal plane. The ALEXO exoskeleton has a total of 8 DOFs. The hip joint of the ALEXO has two DOFs: one active DOF in the sagittal plane to provide external active assistive torque, and a passive DOF for adduction and abduction. The knee joint has one active DOF

for flexion and extension. The ankle joint is passive to accommodate dorsiflexion and plantar flexion.

The exoskeleton is adaptable to different body types and can adjust shank length, thigh length, hip width, and interchange user attachment option depending on user needs. Furthermore, adjustable mechanical end-stops are present in the system to ensure user safety. The range of motion of the joint angles are shown in Table 1, which is sufficient to accommodate the lower human motion.

Table 1. Angular range of motion(ROM) and DOF of joints

Joint	DOF	Freedom Type	ROM
Hip	Flexion/Extension	Active	95°/25°
-	Adduction/Abduction	Passive	10°/15°
Knee	Flexion/Extension	Active	90°/0°
Ankle	Dorsiflexion/Plantar Flexion	Passive	20°/45°

The mechanical structures of ALEXO are made of 6061 and 7075 aluminum alloy. The light-weighted segments decrease the system's inertia. Four 3D-printed TPA cuffs attach to the thigh part and the shank part of both legs to fixate and align the human body in the exoskeleton. Each cuff consists of two curved segments, one in the front and one in the back, which is connected to an adjustable slide rail to adjust for different thigh and shank sizes. Elastic straps are used to tighten the cuffs. ALEXO is supported from the ground by two glass fiber foot attachments. Four Maxon EC60 48V 100W flat motors are selected for hip and knee joints. The motors drive integrates back-driveable harmonic gear drives with a ratio of 1:120 for the hip and 1:50 for the knee joint, respectively.

2.2 Hardware and Control Architecture

The hardware and control architecture of ALEXO are illustrated in Fig. 2. The system consists of two Teensy 4.1 micro controller boards that are serially connected to a PC. Each Teensy is connected to a leg and processes data from its hip and knee joint. In particular, each Teensy is connected to two ESCON 50/5 servo controllers, two Broadcom AEAT 6012 absolute encoders, and two HX711 load cell amplifiers. The Broadcom encoders are attached to the non-drive side of ALEXO and read the joint angle of the hip and knee directly from the pilot side of the exoskeleton.

ALEXO is operated on a hierarchical control. The high-level control is implemented on the Teensy 4.1 micro controllers. A computer connected serially to each Teensy has a user interface in which data is received and monitored in real time. By having a high-speed data serial data communication (5 *ms* cycle time) between the ESCON controller and sensors, the Teensy boards can compute reference trajectories and send these to the low-level ESCON 50/5 servo controller.

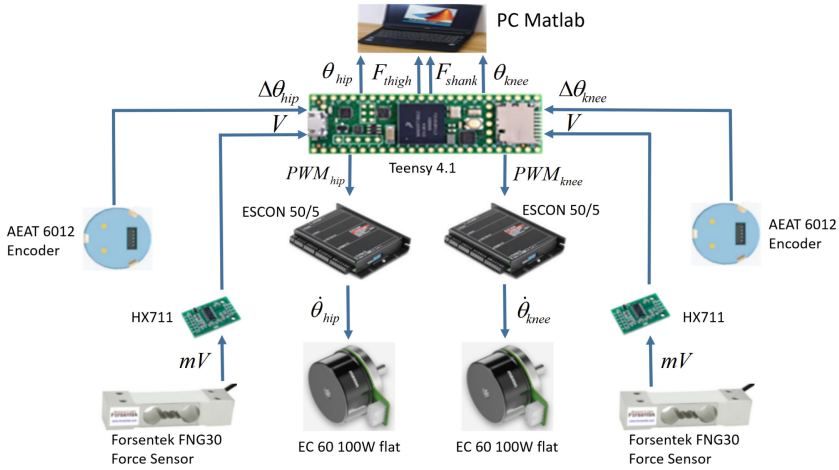


Fig. 2. The hardware and control architecture of a single leg in ALEXO

3 Trajectory Control Method

As the leg segments of the ALEXO follow the human lower limb motion with 2-DOF active, the robot movement can be described as a two-link system. Figure 3 illustrates the ALEXO exoskeleton dynamic model.

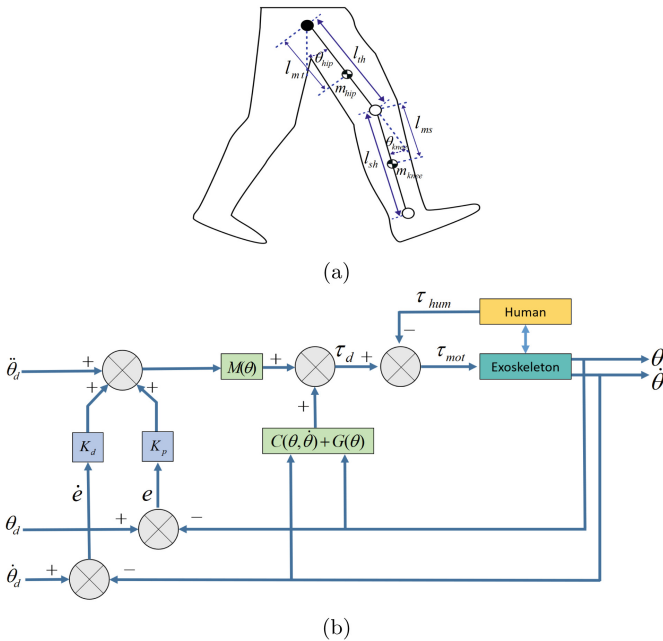


Fig. 3. (a) ALEXO exoskeleton dynamic model. (b) The control scheme of the ALEXO.

The nonlinear dynamics of the ALEXO exoskeleton interacting with the user is given as:

$$M(\theta)\ddot{\theta} + C(\dot{\theta}, \theta)\dot{\theta} + G(\theta) = \tau_{mot} + \tau_{hum} \quad (1)$$

where $M(\theta)$ is the inertial matrix, $C(\dot{\theta}, \theta)$ represents the matrix of Coriolis and centrifugal force, $G(\theta)$ donates the gravitational effect, $\theta = [\theta_{hip} \ \theta_{knee}]^T$, where θ_{hip} and θ_{knee} represent the hip joint and the knee joint of the exoskeleton respectively, τ_{mot} and τ_{hum} are torques from the exoskeleton and the human joint, respectively.

As shown in Fig. 3, a CTC trajectory control is proposed for the exoskeleton:

$$\tau_{mot} = M(\theta)(\ddot{\theta}_d + K_p e(t) + K_d \dot{e}(t)) + C(\dot{\theta}, \theta)\dot{\theta} + G(\theta) - \tau_{hum} \quad (2)$$

$$e(t) = \theta_d(t) - \theta(t) \quad (3)$$

where $\theta_d(t) = [\theta_{d,h}, \theta_{d,k}]$ represents the predefined target position of hip and knee joints; e is the difference between desired angular position and actual angle, K_p and K_d are the proportional and the derivative gains of the CTC controller.

ESCON controllers adopt velocity control. Considering the walking movement pattern, the desired velocity is written as:

$$\int_0^t \ddot{\theta}_r(t) dt = \dot{\theta}_r(t) \quad (4)$$

$\ddot{\theta}_r(t)$ are the desired acceleration, which can be described as:

$$\ddot{\theta}_r(t) = M^{-1}(\tau_{mot} - C(\dot{\theta}, \theta)\dot{\theta} - G(\theta) + \tau_{hum}) \quad (5)$$

thus eq. (4) can be described as:

$$\dot{\theta}_r(t) = \int_0^t M^{-1}(\tau_{mot} - C(\dot{\theta}, \theta)\dot{\theta} - G(\theta) + \tau_{hum}) dt \quad (6)$$

4 Simulations

Simulations are conducted on MATLAB. For simulating the interaction forces, two forces, F_t and F_s that are applied on the thigh and shank, are written as:

$$F_t = 50 \cos(\omega t) - 50 + f_t \quad (7a)$$

$$F_s = 40 \cos(\omega t) - 40 + f_s \quad (7b)$$

where ω is set to π , f_t and f_s are random disturbance ranging from 0 to 10 N. The mass distribution of the ALEXO and the parameters of the controller gain are shown in Table 2.

The sinusoidal reference trajectories of the hip joint and the knee joint are given as:

$$\theta_h = 60 \sin(\pi t - 0.194\pi) + 35 \quad (8a)$$

$$\theta_k = 45 \cos(\pi t) - 45 \quad (8b)$$

The results are shown in Fig. 4. The maximum errors of trajectory tracking for the hip and knee joints are 1.50 and 2.20 °C, respectively.

Table 2. Control parameters.

	Hip	Knee
K_p	3600	6400
K_d	110	140

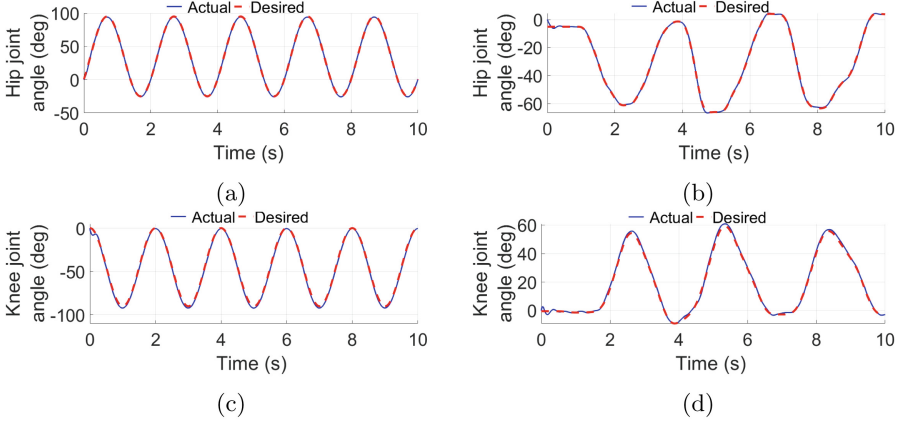


Fig. 4. Trajectory tracking simulation results: (a) hip joint with sinusoidal trajectory, (b) hip joint with real gait, (c) knee joint with sinusoidal trajectory, (d) knee joint with real gait.

5 Physical Experiments

5.1 Trajectory Tracking

The control algorithm was firstly tested on the ALEXO without users. The exoskeleton was fixed on the aluminum alloy frame, and sinusoidal trajectories were applied to the hip and the knee joints:

$$\theta_{dh} = 15 \sin(\omega t), \theta_{dk} = 25 \sin(\omega t) + 25 \quad (9)$$

The results of the sinusoidal trajectory following are shown in Fig. 5. Larger errors are shown at the beginning of the trajectory while smaller errors appear during the trajectory tracking mode, but the level of errors is generally acceptable.

A real walking gait trajectory was also used to test the performance of the trajectory tracking controller. The trajectory is obtained by putting the exoskeleton leg on the human subject and collecting joint sensor data in transparent mode. The results are shown in Fig. 5b and Fig. 5d, respectively. Although there were some errors on the knee joint, the whole exoskeleton robot had a good performance on trajectory tracking to realize walking gait.

5.2 Walking Assistance Tests

The proposed method was evaluated on walking assistance with the ALEXO robot. Experiments were performed on a single subject with height of 179 cm and weight of 65 kg. The subject was required to walk on the treadmill wearing the ALEXO working on the trajectory tracking mode (Fig. 1c). Interaction force between the exoskeleton and the human body was collected during walking.

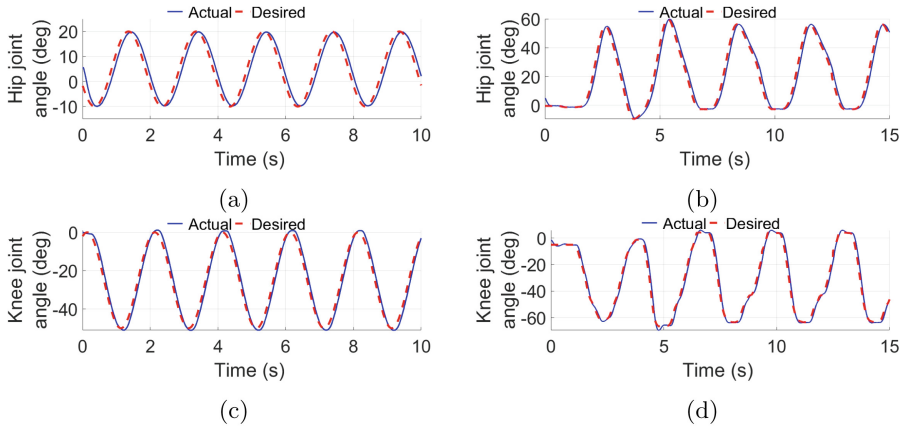


Fig. 5. Trajectory tracking results: (a) hip joint with sinusoidal trajectory, (b) hip joint with real gait, (c) knee joint with sinusoidal trajectory, (d) knee joint with real gait.

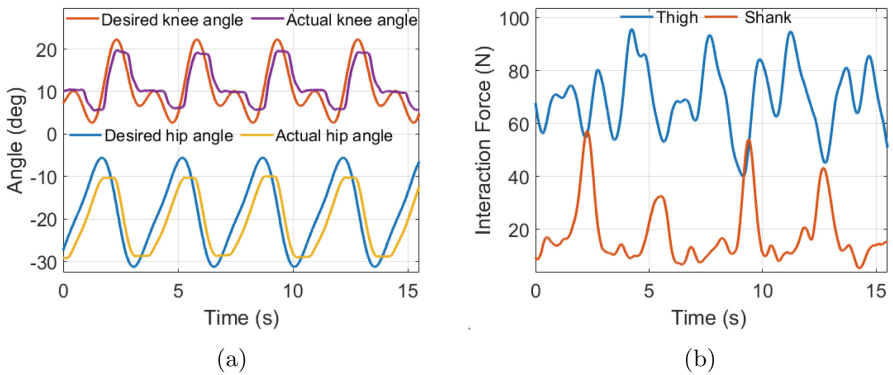


Fig. 6. Human-exoskeleton interaction test with real walking gait trajectory. (a) Angles of hip and knee joints. (b) Interaction force values of the lower limb.

As shown in Fig. 6, the exoskeleton follows the desired trajectory, while providing assistive force to the subject. Periodical force patterns can be observed during the gait cycle on the thigh and the shank segments. Maximum interaction forces of 95.83 N and 57.29 N were measured at the thigh and the shank, respectively.

6 Conclusions

This paper presents the design of an active lower limb exoskeleton (ALEXO) for walking assistance. A trajectory tracking control method is proposed, which has been simulated and tested with the physical system. Our experiments demonstrated that the ALEXO was able to provide sufficient assistance on the hip and knee joints during walking to follow a given gait.

Future work will focus on improving the control method to achieve adaptive gait control for different users. The effectiveness of the ALEXO in assisting individuals with different walking patterns will be evaluated through user studies. Furthermore, the motion primitives theory will be applied to the ALEXO, which can contribute to achieving gait control that is more robust and intelligent.

Acknowledgments. The authors acknowledge the financial support by the Frode V. Nyegaards and Wife's fund for the ALEXO project.

References

1. Nam, K.Y., Kim, H.J., Kwon, B.S., et al.: Robot-assisted gait training (Lokomat) improves walking function and activity in people with spinal cord injury: a systematic review. *J. NeuroEng. Rehabil.* **14**(1), 1–13 (2017)
2. Husty, M., Birlescu, I., Tucan, P., et al.: An algebraic parameterization approach for parallel robots analysis. *Mech. Mach. Theory* **140**, 245–257 (2019)
3. Grazi, L., Trigili, E., Proface, G., et al.: Design and experimental evaluation of a semi-passive upper-limb exoskeleton for workers with motorized tuning of assistance. *IEEE Trans. Neural Syst. Rehabil. Eng.* **28**(10), 2276–2285 (2020)
4. Bai, S., Virk, G.S., Sugar, T.: *Wearable exoskeleton systems: design, control and application*. The Institution of Engineering and Technology (2018)
5. Tu, Y., Zhu, A., Song, J., et al.: Design and experimental evaluation of a lower-limb exoskeleton for assisting workers with motorized tuning of squat heights. *IEEE Trans. Neural Syst. Rehabil. Eng.* **30**, 184–193 (2022)
6. Liu, J., Zhang, Y., Wang, J., et al.: Adaptive sliding mode control for a lower-limb exoskeleton rehabilitation robot. In: *IEEE Conference on Industrial Electronics and Applications*, pp. 1481–1486 (2018)
7. Meijneke, C., van Oort, G., Sluiter, V., et al.: Symbitron exoskeleton: design, control, and evaluation of a modular exoskeleton for incomplete and complete spinal cord injured individuals. *IEEE Trans. Neural Syst. Rehabil. Eng.* **09**, 330–339 (2021)
8. Patané, F., Rossi, S., Sette, F.D., et al.: WAKE-Up exoskeleton to assist children with cerebral palsy: design and preliminary evaluation in level walking. *IEEE Trans. Neural Syst. Rehabil. Eng.* **25**(7), 906–916 (2017)
9. Wang, X., Guo, S., Song, M., et al.: Mechanical design and experimental verification of a parallel hip exoskeleton with virtual rotation center. In: *IEEE International Conference on Advanced Robotics and Mechatronics*, pp. 230–235 (2021)
10. Simonsick, E.M., Newman, A.B., Visser, M., et al.: Mobility limitation in self-described well-functioning older adults: importance of endurance walk testing. *J. Gerontol. Ser. A* **63**(8), 841–847 (2013)

11. Zhou, X., Yu, Z., Wang, M., et al.: Design of control system for lower limb exoskeleton robot. In: International Conference on Control, Automation and Robotics, pp. 122–126 (2022)
12. Peng, X., Acosta-Sojo, Y., Wu, M., et al.: Actuation timing perception of a powered ankle exoskeleton and its associated ankle angle changes during walking. *IEEE Trans. Neural Syst. Rehabil. Eng.* **30**, 869–877 (2022)
13. Colins, S.H., Wiggin, M.B., Sawicki, G.S.: Reducing the energy cost of human walking using an unpowered exoskeleton. *Nature*. **522**(7555), 212–215 (2015)
14. Véronneau, C., Bigué, J.L., Lussier-Desbiens, A., et al.: A high-bandwidth back-drivable hydrostatic power distribution system for exoskeletons based on magnetorheological clutches. *IEEE Robot. Autom. Lett.* **3**(3), 2592–2599 (2018)
15. Galle, S., Malcolm, P., Collins, S.H., et al.: Reducing the metabolic cost of walking with an ankle exoskeleton: interaction between actuation timing and power. *J. Neuroeng. Rehabil.* **14**, 35 (2017)
16. Kawamoto, H., Kandone, H., Sakurai, T., et al.: Development of an assist controller with robot suit hal for hemiplegic patients using motion data on the unaffected side. In: International Conference of the IEEE Engineering in Medicine and Biology Society, pp. 3077–3080 (2014)
17. Zhang, A., Tu, Y., Zheng, W., et al.: Adaptive control of man-machine interaction force for lower limb exoskeleton rehabilitation robot. In: IEEE International Conference on Information and Automation, pp. 740–743 (2018)
18. Huang, R., Cheng, H., Guo, H., et al.: Hierarchical interactive learning for a human-powered augmentation lower exoskeleton. In: IEEE International Conference on Robotics and Automation, pp. 257–263 (2016)
19. Schrade, S.O., Nager, Y., Wu, A.R., et al.: Bio-inspired control of joint torque and knee stiffness in a robotic lower limb exoskeleton using a central pattern generator. In: International Conference on Rehabilitation Robotics, pp. 1387–1394 (2017)
20. Gui, K., Liu, H., Zhang, D.: A generalized framework to achieve coordinated admittance control for multi-joint lower limb robotic exoskeleton. In: International Conference on Rehabilitation Robotics, pp. 228–233 (2017)
21. Christensen, S., Rafique, S., Bai, S.: Design of a powered full-body exoskeleton for physical assistance of elderly people. *Int. J. Adv. Rob. Syst.* **18**(6), 1–15 (2021)
22. Bai, S., Islam, M.R., Power, V., et al.: User-centered development and performance assessment of a modular full-body exoskeleton (AXO-SUIT). *Biomim. Intell. Robot.* **2**(2), 100032 (2022)